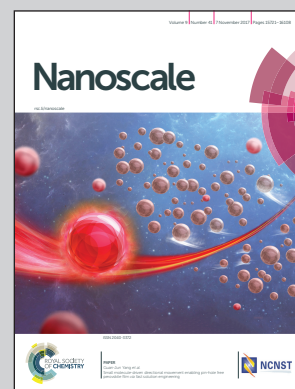


Showcasing research from the CAS Key Laboratory of Mechanical Behavior and Design of Materials, University of Science and Technology of China, Hefei, Anhui, 230026, P. R. China.

A Janus oil barrel with tapered microhole arrays for spontaneous high-flux spilled oil absorption and storage

Frequent oil spill accidents have caused severe damage to the ecosystems of oceans and coastlines. This work provides a novel Janus oil barrel (superhydrophobic outside wall and superhydrophilic inside wall) constituted by tapered microhole arrayed aluminium foil, which can spontaneously absorb spilled oil and synchronously store the absorbed oil with high flux and unidirectional transferability. In addition, the barrel can absorb oil from surfactant-free oil-in-water emulsions. This distinct design combining femtosecond laser micro/nanofabrication technology provides a promising strategy for oil spill remediation.

As featured in:



See Guoqiang Li, Dong Wu et al., *Nanoscale*, 2017, 9, 15796.




rsc.li/nanoscale

Registered charity number: 207890



Cite this: *Nanoscale*, 2017, **9**, 15796

A Janus oil barrel with tapered microhole arrays for spontaneous high-flux spilled oil absorption and storage†

Zhen Zhang,^{a,b} Yinghui Zhang,^a Hua Fan,^c Yulong Wang,^a Chen Zhou,^d Feifei Ren,^e Sizhu Wu,^d Guoqiang Li,^{*a,f} Yanlei Hu,^a Jiawen Li,^a Dong Wu  ^{*a} and Jiaru Chu^a

Porous oil/water separation materials show excellent prospects in the remediation of oil spill accidents. However, several drawbacks such as low flux, limited absorption and storage capacity restrict their practical applications. Hence, a novel Janus oil barrel (superhydrophobic outside wall and superhydrophilic inside wall) constituted by tapered microhole arrayed aluminium foil is designed, which is demonstrated to be a promising device for the remediation of oil spill accidents. Furthermore, the investigation shows that the tapered microholes (taper angle 25–30°) can significantly enhance oil/water intrusion pressures (1–3 times higher than cylindrical holes) and unidirectional transferability which can eliminate the secondary leakage when salvaging full oil barrels without an additional procedure. It is indicated that the Janus oil barrel can spontaneously absorb spilled oil with a high flux (45 000 L m⁻² h⁻¹), and synchronously store the absorbed oil. In addition, the barrel can absorb oil from surfactant-free oil-in-water emulsions appearing in oil spills and industrial processes. The distinct design combining excellent controllability, high precision and flexibility of the femtosecond laser micro/nanofabrication technology provides a general strategy in oil spill remediation.

Received 30th May 2017,
Accepted 17th July 2017
DOI: 10.1039/c7nr03829a

rsc.li/nanoscale

1. Introduction

Frequent oil spill accidents have caused severe damage to the ecosystems of oceans and coastlines, and how to recycle the spilled oil on water is a timely and urgent worldwide concern.^{1–3} Due to their excellent prospects such as high efficiency and high flux, metal meshes,^{3–6} sponges,^{7–9} foams,^{10,11} membranes^{12,14–22} and even sand²³ have been employed for oil/water separation. But these materials suffer from uncontrollable internal structures, limited absorption

and storage capacity.^{13,24,26–28} To address these issues, Ge *et al.*¹⁰ designed an oil collection apparatus based on a simple combination of porous hydrophobic and oleophilic materials (PHOMs) with pipes and a self-priming pump to realize consecutive collection of oil from the water surface. Although this strategy has promising applications in large-area oil spill remediation, it needs additional equipment such as pumps and ships.

It is reported that Janus systems (Janus cotton fabric,¹⁴ membrane,¹⁵ and graphene oxide sponge⁷) have been successfully utilized to separate oil-in-water or water-in-oil emulsions with high speed and purity. However, these Janus materials have non-uniform holes and tedious reaction steps, leading to smaller intrusion pressure and limited production. And the unidirectional transferability has not been mentioned. Hence, it is of great significance to seek a novel device for high-flux oil spill remediation containing oil on water and oil in emulsion recycling. In this work, a kind of distinct Janus aluminum foil with tapered microhole arrays can be constructed by laser drilling, fluorination modification and selective removal. This Janus barrel is designed as superhydrophobic/superoleophilic on the outer surface and superhydrophilic/underwater superoleophobic on the inner surface. These unique tapered microholes are beneficial for enhancing the supportable intrusion pressure and avoid the secondary leakage when salvaging the

^aCAS Key Laboratory of Mechanical Behavior and Design of Materials, Department of Precision Machinery and Precision Instrumentation, University of Science and Technology of China, Hefei, Anhui, 230026, P. R. China. E-mail: guoqli@ustc.edu.cn, dongwu@ustc.edu.cn

^bCAS Key Laboratory of Geospace Environment, USTC, Hefei 230026, China

^cDepartment of Mechanical and Electronic Engineering, Hefei University of Technology, Hefei, Anhui, 230009, P. R. China

^dSchool of Instrument Science and Opto-electronics Engineering, Hefei University of Technology, Hefei, Anhui, 230009, P. R. China

^eSchool of Electrical Engineering and Automation, Anhui University, Hefei, Anhui, 230601, P. R. China

^fKey Laboratory of Testing Technology for Manufacturing Process of Ministry of Education, Southwest University of Science and Technology, Mianyang 621010, P. R. China

†Electronic supplementary information (ESI) available. See DOI: 10.1039/c7nr03829a

full oil barrel. The barrel with controllable microhole arrays shows abilities of spontaneously absorbing spilled oil with high flux, large capacity, unidirectional transferability, and eliminating secondary leakage without an additional procedure. Besides, surfactant-free oil-in-water emulsions can also be separated by this kind of Janus barrel. It is worth mentioning that this work provides a novel strategy for the remediation of oil spill accidents and also inspires broad applications such as fog collection, particle filtration, fluid micro-valve and so forth.

2. Experimental section

Materials

Aluminum foil (thickness 35 μm) was purchased from New Metal Material Tech. Co., Ltd, Beijing, China. The oils used for simulating oil spill are normal octane (C_8H_{18}) and 1,2-dichloroethane ($\text{C}_2\text{H}_4\text{Cl}_2$) which were purchased from Sinopharm Chemical Reagent Co. Ltd, Shanghai, China.

Fabrication of Janus microhole arrayed aluminum foil

Aluminum foil with uniform microhole arrays was fabricated by using a regenerative amplified Ti:sapphire femtosecond laser system (Legend-Elite-1K-HE, Coherent, USA) that generates 104 fs pulses at a repetition rate of 1 kHz with a central wavelength of 800 nm. The drilling process was controlled by using a 2D scanning galvanometer (Scanlab GamH, hurrySCAN II 10, Germany). The diameter of the focus spot on the aluminum foil is about 20 μm . The microholes with diameters from 14.05 to 31.3 μm are fabricated by precisely controlling the laser pulse energy from 0.6 μJ to 4 μJ , and the pulse number from 30 to 50, while bigger holes are fabricated by laser scanning in a circular path. The interval between adjacent holes is kept at 100 μm . A microhole arrayed aluminum foil with the total size of 9.3 cm \times 3.1 cm and with the interval of 100 μm can be fabricated in \sim 3 hours. The microholed aluminum foil is superhydrophilic (upper surface and lower surface) after laser drilling. Then, the superhydrophilic aluminum foils are modified to become superhydrophobic by low surface energy 1H,1H,2H,2H-perfluorodecyltriethoxysilane (PFDTES). After that, the lower surface is scanned by using a laser at a speed of 15 mm s^{-1} , a pulse energy of 0.75 μJ and a scanning space of 20 μm , and becomes superhydrophilic, while the upper surface and the inner wall of micro-holes remain superhydrophobic. Finally, the Janus barrel is assembled by using microholed aluminum foil and glass molds. The aluminum foil does not need to be attached to other substrates, and a metallic skeleton should be used to assemble a larger barrel for promoting the ruggedness.

Instrument and characterization

The morphologies of microhole arrayed aluminum foil surfaces were observed by using a scanning electron microscope (SEM, JSM-6700F, JEOL, Tokyo, Japan). The 5 μL water and oil contact angles (WCAs and OCAs) were measured by using a contact-angle system (CA100D, Innuo, China). The average

value of five measurements performed at different locations on the same sample was adopted as the contact angle.

Oil spill remediation and oil-in-water emulsion separation experiments

For oil spill remediation, 30 mL normal octane dyed with Sudan III was poured into 600 mL water dyed with methylene blue. Before the Janus barrel was put in the mixture, the inside surface of the barrel was pre-wet by a little water. Four samples of microholed aluminum foil with hole diameters of 14.05, 19.3, 31.3, and 40.3 μm were assembled to four Janus barrels. For oil-in-water emulsion separation, C_8H_{18} and $\text{C}_2\text{H}_4\text{Cl}_2$ are mixed with a ratio of 1.1 : 1.5. Firstly, 26 mL mixed oil was poured into 500 mL water in a beaker. Then, the oil/water mixture was stirred by using a magnetic stirrer at a speed of 400 rpm for 2 min to prepare an oil-in-water emulsion. After that, a Janus oil barrel was put into the emulsion at a stirring speed of 200 rpm. Finally, oil would be absorbed into the Janus oil barrel.

3. Results and discussion

Janus tapered microhole arrays on aluminum foils are fabricated orderly by femtosecond laser micro-drilling,^{29,30} surface fluorination, and fluorination removal on the lower surface, as shown in the schematic fabrication steps of Fig. 1a. Microhole arrays with high uniformity (error is less than 0.15 μm measured from the SEM images) have been fabricated after the 1st step.²⁹ Then in the 2nd step, the double-faced superhydrophilic microholed aluminum foil was modified to become double-faced superhydrophobic by low surface energy 1H,1H,2H,2H-perfluorodecyltriethoxysilane (PFDTES). The corresponding WCAs at different steps are shown in Fig. 1b. Janus microholed aluminum foil was obtained after the 3rd step by laser scanning at 15 mm s^{-1} speed, 20 μm scanning space, and 0.75 μJ pulse energy to overcome fluorination on the lower surface. Because of the tapered hole, the laser scanning would not damage the inner wall of the microholes and the upper surface. As shown in the SEM images in Fig. 1b, the upper surface is covered by micro-fragments (2 to 10 μm) around the hole, while the lower surface is covered by micro-protuberances (0.2 to 1 μm). After the 3rd step, the lower surface became superhydrophilic (\sim 154.7 $^\circ$ to \sim 4.2 $^\circ$) while the upper surface remained superhydrophobic (\sim 166.7 $^\circ$ to \sim 158.4 $^\circ$) [Fig. 1b]. In addition, the changes of OCAs in air and water after the three processing steps are shown in Table S1 in the ESI.† In general, the single layer Janus foil shows not only different morphologies but also different wettabilities on the two sides.

Due to the flexibility of aluminum foil, an oil barrel can be assembled with Janus microholed aluminum foil. The schematic processes are shown in the 4th and 5th steps in Fig. 1a, and the pictures are shown in Fig. S1 in the ESI.† Home-made glassware is used to match up the Janus microholed aluminum foil with a size of 93 \times 31 mm², and the rubber plug can

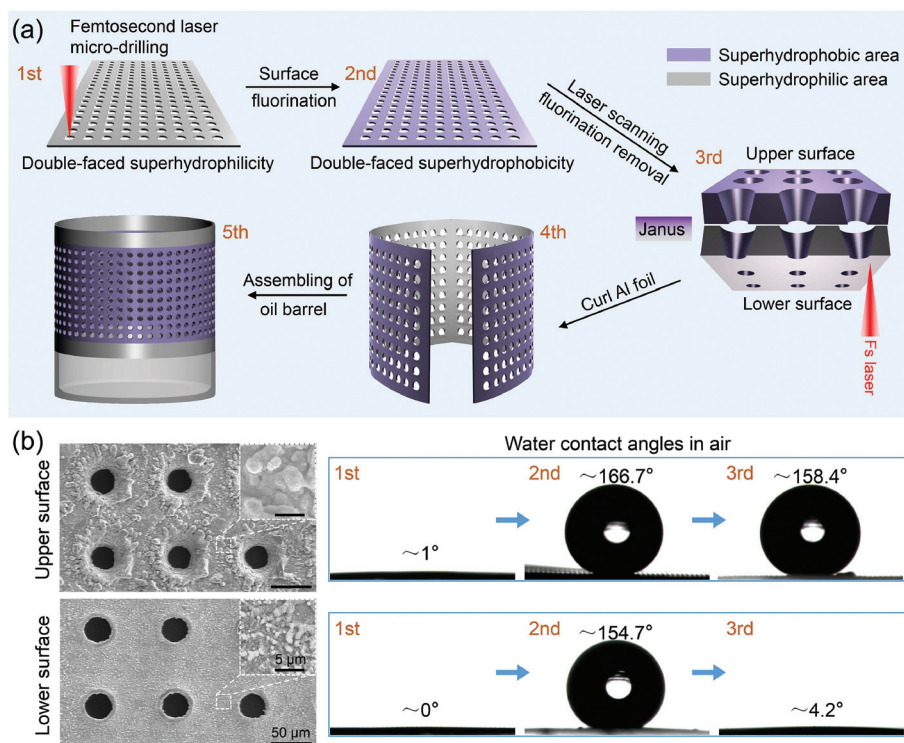


Fig. 1 Programmed laser micro-drilling, modification, scanning and assembling processes to fabricate a Janus barrel with tapered hole arrays. (a) The schematic illustration of fabricating the Janus microhole arrayed aluminum foil and assembling the Janus barrel. The 1st step is micro-drilling by using a femtosecond laser. The 2nd step is surface modification with perfluorodecyltriethoxysilane. The 3rd step is laser scanning on the lower surface to overcome fluorination. The 4th and 5th steps are assembling the Janus microholed aluminum foil with other units. (b) The SEM images of the upper and lower surfaces with microhole arrays after the 3rd step. The upper surface is covered by micro-fragments with diameters from 2 to 10 μm which are bigger than the micro-protuberances (0.2 to 1 μm) on the lower surfaces. (c) The contact-angle images of the upper and lower surfaces after different steps. Janus microhole arrayed foil is obtained after the 3rd step.

maintain the balance of the barrel on the water surface (ESI, Fig. S1†). Hence, the Janus oil barrel with superhydrophobicity/superoleophilicity on the outside wall and superhydrophilicity/under water superoleophobicity on the inside wall can be constructed.

Fig. 2a shows four samples of microhole arrays with the same interval of 100 μm and different hole diameters (D_1/D_2 : 14.05/31.8, 19.3/37.8, 31.3/47, and 40.3/56.9 μm), which can be adjusted by altering the laser pulse energy and pulse number. Additionally, the cross-section SEM images in Fig. 2b demonstrate the tapered morphology of the microholes which is caused by the Gaussian laser ablation, and the inset shows micro/nano-wrinkles on the inner wall of the hole. The taper angle α is an important parameter to characterize the tapered hole, which can be described as eqn (1)

$$\alpha = 2 \tan^{-1}(D_1 - D_2)/2H \quad (1)$$

where D_1 , D_2 , and H are the biggest hole diameter, the smallest hole diameter, and the thickness of aluminum foil, respectively. All these parameters have also been labeled in Fig. 2c. The statistical results of hole diameters and taper angles are shown in Fig. 2d and e. With the increase of hole diameters

(samples 3 and 4), the taper angles show a slight decline due to the increased pulse number or pulse energy.

The Janus oil barrel can be fabricated by assembling microhole arrayed aluminum foil. The Janus barrel can solve problems of limited oil absorption and storage capacity that were difficult to solve before. Furthermore, the superhydrophobic outside wall will stop water from entering into the barrel and the underwater superoleophobic inside wall will prevent the absorbed oil from leaking out. In order to verify this concept, a Janus oil barrel with a height of 85 mm and a diameter of 35 mm which consisted of a microhole diameter of 40.3 μm and an interval of 100 μm was fabricated to perform the collection of spilled oil. Here, C_8H_{18} was chosen as the target oil and then 30 mL dyed oil (red) was poured into 600 mL dyed water (blue) [Fig. 3a]. As shown in Fig. 3a (side view) and 3b (top view), at $T = T_0$, the barrel was put into the baker after pouring into the oil. Then the absorption proceeded spontaneously under the capillary force. At $T = 33$ s, almost all the spilled oil was absorbed into the barrel. From the side view in Fig. 3a, the empty barrel was gradually filled by absorbed oil and no water would be absorbed due to the superhydrophobic outside wall of the barrel. From the top view in Fig. 3b, the muddy oil/water mixture became very clear after 33 s [ESI, Movies S1 and S2†]. The absorption speeds of the Janus oil barrel with different

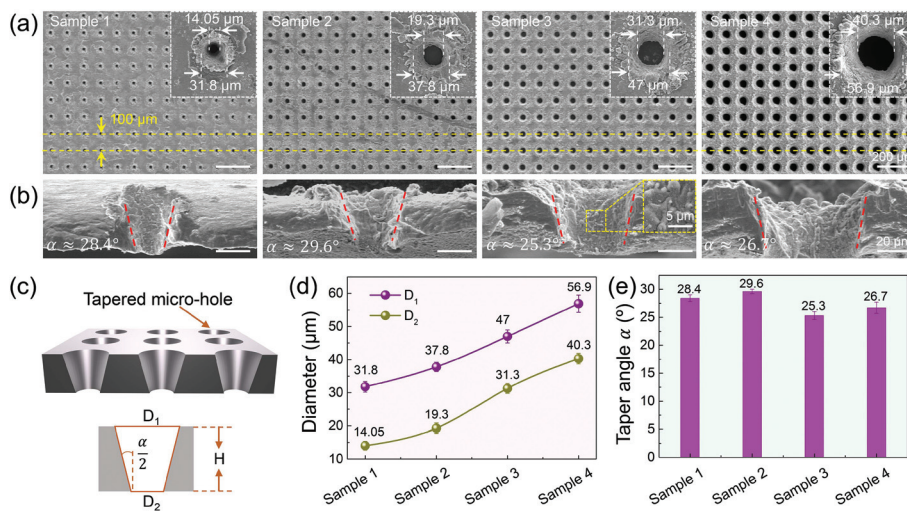


Fig. 2 Janus tapered microhole arrays with different diameters. (a) and (b) are the top-view and cross-section SEM images of tapered microholes. The microholes with diameters from 14.05 to 31.3 μm are fabricated by precisely controlling the laser pulse energy from 0.6 μJ to 4 μJ , and the pulse number from 30 to 50, while bigger holes are fabricated by laser scanning in a circular path. (c) 3D schematic and its cross-section of the tapered microhole; where D_1 , D_2 , H and α are the biggest diameter, the smallest diameter, the thickness of the aluminum foil and the taper angle of the tapered microholes, respectively. (d) The hole diameters on the upper and lower surfaces in four samples. (e) The taper angles of the microholes in four samples.

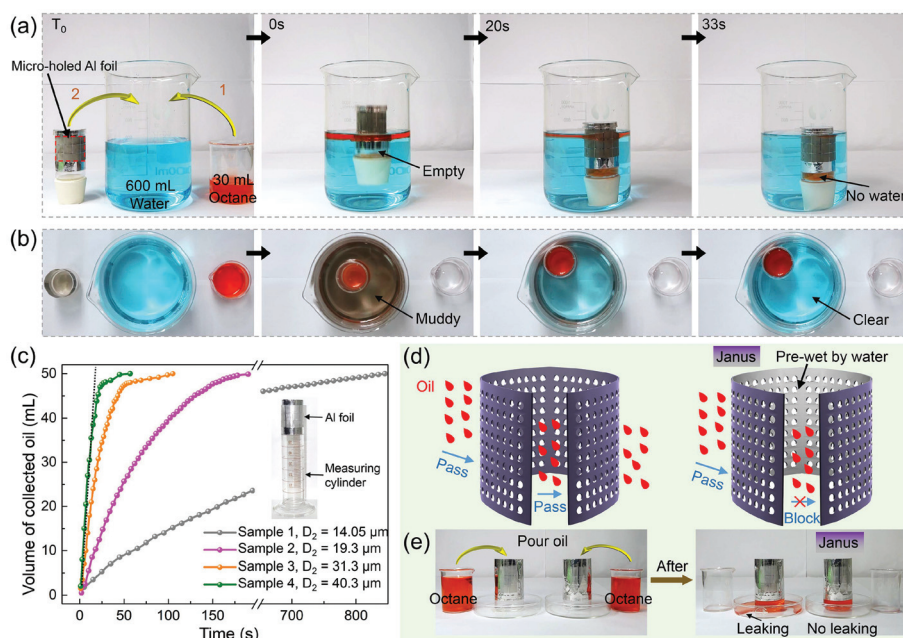


Fig. 3 Fast absorption and anti-leakage of Janus oil barrels. (a) and (b) are side-view and top-view of the time-lapse images of the spilled oil absorption. The Janus barrels absorb spilled oil with high flux ($45\,000\ \text{Lm}^{-2}\ \text{h}^{-1}$ in sample 4) and efficiency. The volumes of the spilled oil are 30 mL. (c) The volume of absorbed oil as a function of time in different hole diameters. (d) and (e) are the schematic illustration and optical images of the comparison between the double-faced superhydrophobic barrel and the Janus barrel, respectively. The Janus barrel shows the ability to prevent the absorbed oil from leaking outside.

hole diameters were systematically obtained by using a measuring cylinder (the inset of Fig. 3c) which was stuck in the bottom of a beaker (Fig. S2†). As shown in Fig. 3c, the oil barrel with a bigger hole diameter possesses a higher absorption speed. Although the volume of the absorbed oil increased

non-linearly due to the limited spilled oil, the absorbed oil increased almost linearly before 20 s in sample 4. So, the average flux of the Janus oil barrel with a hole diameter of 40.3 μm is about $45\,000\ \text{Lm}^{-2}\ \text{h}^{-1}$, demonstrating the excellent performance of the remediation of oil spill accidents.

Oil can be absorbed into the double-faced superhydrophobic barrel and can also flow out from the barrel. While the absorbed oil will be blocked by the pre-wetted superhydrophilic microholed aluminum foil surface, hence oil cannot flow out of the Janus oil barrel. The schematic illustrations are shown in Fig. 3d. The comparison between the Janus oil barrel and the double-faced superhydrophobic oil barrel is also conducted as shown in Fig. 3e and Movie S3 in the ESI.† These results showed that the Janus oil barrel can effectively eliminate secondary leakage without an additional procedure.

Oil spill accident remediation involves not only absorbing floating oil, but also absorbing a small number of oil droplets from oil-in-water emulsions which were generated by the oscillation of water. As shown in Fig. 4a and Movie S4,† during the magnetic stirrer stirring, 26 mL dyed oil (red) was absorbed into the barrel from surfactant-free oil-in-water emulsions in less than 23 min. Clearer water and increasing absorbed oil demonstrated that the Janus oil barrel can absorb oil from oil-in-water emulsions effectively. The insets in Fig. 4a show the decrease of oil drops and Fig. 4b shows the diameter distributions of oil drops as a function of time. Bigger oil drops are preferentially absorbed by the barrel due to the higher probability of coming in contact with the barrel. Interestingly, four samples with different microhole diameters exhibit little difference in absorption times that are between 22 min and 26 min (Fig. 4c). The reason is that the four aluminum foil samples have similar areas of superoleophilic surfaces. Hence, the Janus oil barrel shows dual ability: floating oil on water and oil in surfactant-free oil-in-water emulsion collection.

Actually, as shown in Fig. 5a, two kinds of Janus systems can be fabricated by removing fluorination on the upper (a1) and lower (a2) surfaces, respectively. System a1 is constituted by the superhydrophilic inner wall of the microholes, superhydrophilic upper surface, and the superhydrophobic lower

surface, while system a2 is constituted by the superhydrophobic inner wall of the microholes, superhydrophobic upper surface, and the superhydrophilic lower surface. We found that only a2 can be utilized in oil spill accident remediation, and the possible reason is that the superhydrophobic microhole can withstand a higher height for water and oil due to a larger intrusion pressure. The experimental intrusion pressure can be expressed by using eqn (2) and (3)^{5,17,25,29,33}

$$P_{w\text{-exp}} = \rho_w g h_w \quad (2)$$

$$P_{o\text{-exp}} = \rho_o g h_o \quad (3)$$

In eqn (2), $P_{w\text{-exp}}$, ρ_w , h_w , and g are the intrusion pressure of water on the superhydrophobic surface experimentally, the density of water, the maximum height of water that the superhydrophobic microholed aluminum foil can withstand, and the acceleration of gravity, respectively. In eqn (3), $P_{o\text{-exp}}$, ρ_o and h_o are the intrusion pressure of oil on the pre-wet superhydrophilic surface experimentally, the density of oil, and the maximum height of oil that the superoleophobic microholed aluminum foil can withstand, respectively. Meanwhile, the theoretical intrusion pressure can be expressed by using eqn (4) and (5)^{5,25,31,32}

$$P_{w\text{-theor}} \sim 2\gamma_{LV} \cos \theta_{w0} / D \quad (4)$$

$$P_{o\text{-theor}} \sim 2\gamma_{LV} \cos \theta_{o0} / D \quad (5)$$

In eqn (4), $P_{w\text{-theor}}$, γ_{LV} , θ_{w0} , and D are the theoretical intrusion pressure of water on the superhydrophobic surface, the liquid-vapor surface tension, the contact angle of the liquid on the flat aluminum surface and the hole diameter, respectively. In eqn (5), $P_{o\text{-theor}}$, γ_{L1L2} and θ_{o0} are the theoretical intrusion pressure of oil on the pre-wet superhydrophilic surface, the

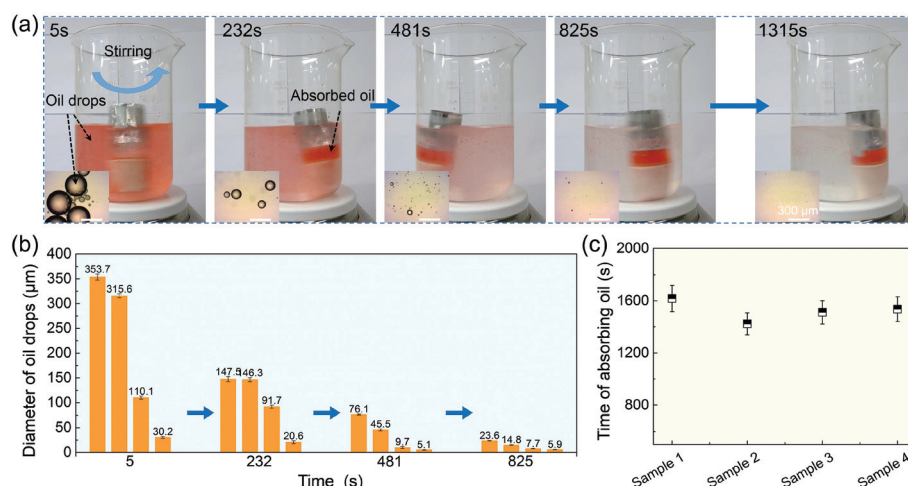


Fig. 4 Absorption of oil from surfactant-free oil-in-water emulsions. (a) The time-lapse images of absorption of oil from oil-in-water emulsions during stirring by using a magnetic stirrer. The insets are microscopy images of oil drops in the baker. (b) The statistical diameters of oil drops as a function of time. Bigger oil drops are preferentially absorbed by the barrel due to the higher probability of coming in contact with the barrel. (c) Absorption times of four Janus oil barrels with different microhole diameters exhibit little difference due to similar areas of superoleophilic outer surfaces.

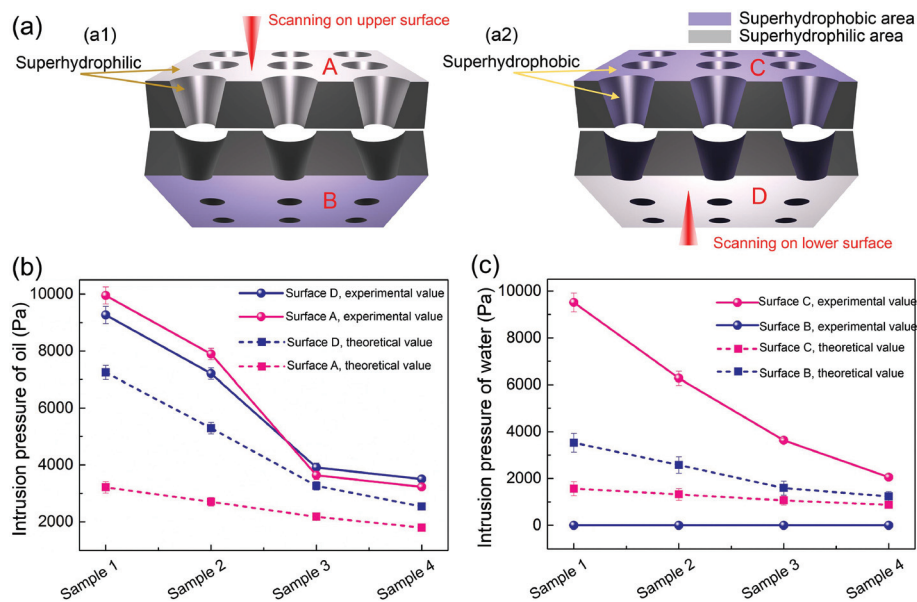


Fig. 5 Intrusion pressure for tapered microholes. (a) Two kinds of Janus systems a1 (superhydrophilic upper surface, superhydrophilic inner wall of microholes, and the superhydrophobic lower surface) and a2 (superhydrophobic upper surface, superhydrophobic inner wall of microholes, and the superhydrophilic lower surface). Only a2 can be utilized in oil spill accident remediation. (b) Theoretical and experimental intrusion pressures of oil on pre-wet superhydrophilic surfaces (surfaces A and D). (c) Theoretical and experimental intrusion pressures of water on superhydrophobic surfaces (surfaces B and C). The tapered microholes serve as a buffer support for withstanding higher water and oil pressures.

water–oil interfacial tension and the oil contact angle on the flat surface, respectively.

Via the comparison of a1 and a2, the intrusion pressures of four surfaces A, B, C and D are calculated in Fig. 5b and c. Theoretically, the microholes can be seen as cylindrical holes, and the intrusion pressure is inversely proportional to the hole diameter. So, the red dotted line (surface A, the biggest hole) in Fig. 5b is always below the blue dotted line (surface D, the smallest hole). Nevertheless, the experimental oil intrusion pressures of surface A (red solid line in Fig. 5b) are bigger than those of surface D (blue solid line in Fig. 5b) in samples 1 and 2, and close to surface D in samples 3 and 4. The reasons are that the tapered microholes serve as a buffer support²³ for withstanding higher oil pressures and the buffer support decreases in samples 3 and 4 due to smaller taper angles (Fig. 2e). In Fig. 5c, the theoretical water intrusion pressures of surface B (blue dotted line, the smallest hole) are higher than those of surface C (red dotted line, the biggest hole) while the experimental water intrusion pressures of surface B are lower than those of surface C due to the tapered hole. Furthermore, the intrusion pressures of surface B are always zero due to the superhydrophilic inner wall of microholes in system a1, leading to an unexpected phenomenon that water passes from surface B to surface A through the microholes [Fig. S3†]. Hence, the superhydrophobic surface in system a1 cannot block water and only a2 can be chosen for assembling the Janus oil barrel. In addition, the tapered holes could support higher water and oil pressures.

From the intrusion pressure of sample 4 in Fig. 5b and c, the water intrusion pressure of surface C is lower than the oil

intrusion pressure of surface D. Hence, the highest height of the barrel depends on the water intrusion pressure of surface C, which is about 20.6 cm from our measurement. However, the diameter of the barrel can be even several meters to increase the volume of the barrel. The consumed time (T_c) of filling up a barrel with oil can be calculated by using eqn (6)

$$T_c = \frac{V}{QS}, \quad (6)$$

where V , Q , and S are the volume of an oil barrel, the average flux of microhole arrayed aluminum foil, and the side area of the oil barrel. If a Janus oil barrel with a bottom diameter of 400 cm and a height of 20.6 cm which consisted of a micro-hole diameter of 40.3 μm and an interval of 100 μm was designed, V is 2600 L, Q is 45 000 $\text{Lm}^{-2} \text{h}^{-1}$, S is 2.6 m^2 , and T_c is 80 s by calculation. An effective strategy for the remediation of oil spill accidents is to throw thousands of Janus oil barrels in ocean, wait for spontaneous oil absorption and storage, and salvage barrels [Fig. 6]. After some cycles, thousands of tons of oil can be recovered in a short time, and the purity can reach up to 99%. Moreover, the barrel can maintain high flux after 10 cycles [ESI, Fig. S4†]. We believe that the designed Janus oil barrel will have promising applications in solving oil spill accidents and many industrial processes.

To achieve continuous recovery of oil, the absorbed oil can be transferred by following the siphon principle. As shown in Fig. 7 and Movie S5 in the ESI,† a Janus oil barrel assembled by microholed aluminum foil and a measuring cylinder was fixed in the bottom of a beaker. Then, a hosepipe was used to connect the barrel and then another beaker was put beneath

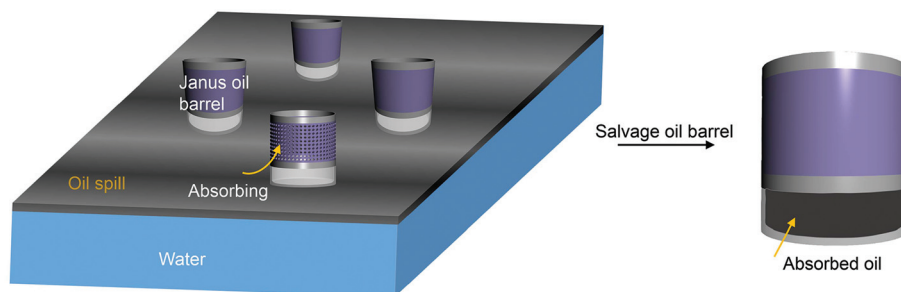


Fig. 6 The schematic illustration of oil spill accident remediation. Three simple steps: throwing thousands of Janus oil barrels in ocean, waiting for spontaneous oil absorption and storage, and salvaging oil barrels.

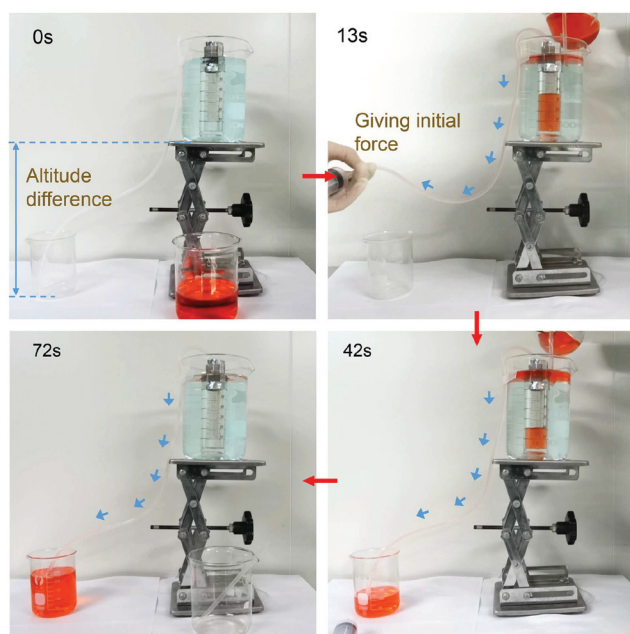


Fig. 7 Transfer of the absorbed oil in the barrel by following the siphon principle. Achievement of consecutive oil recovery without pumping or other continuous power.

the barrel. After that, 200 mL spilled oil was absorbed and transferred in about 72 s. The siphon principle provides a new method to transfer absorbed oil without pumping or other continuous power.

4. Conclusion

In summary, a novel Janus oil barrel (superhydrophobic outside wall and superhydrophilic inside wall) with tapered microhole arrayed aluminum foil was fabricated by femtosecond laser micro-drilling, PFDTES modification, laser scanning on the lower surface and assembling. Because the tapered microholes can significantly enhance the oil/water intrusion pressures and unidirectional transferability, the Janus barrel can eliminate the secondary leakage when salvaging full oil barrels without an additional procedure. As an oil

recovery, the barrel can absorb spilled oil on water and oil in surfactant-free oil-in-water emulsions, which showed high flux, high efficiency, large absorption and storage capacity. In oil spill accidents, oil could be absorbed and stored into our barrels spontaneously, and then the full barrels could be salvaged to recycle oil. The Janus oil barrel with controllable microholes is a good candidate for oil spill accident remediation and industrial oil/water separation. Although the cost of the preparation of the barrel by using the femtosecond laser is very high, larger barrels can be prepared by using a cheap nanosecond laser, high-speed galvanometer and a large-range mobile station for practical application. Furthermore, the method of fabricating a single layer Janus system will inspire new technologies for designing oil/water separators, fog collectors and liquid conveyors.

Acknowledgements

This work is supported by the National Natural Science Foundation of China (no. 51675503, 61475149, 51405464, 61675190, and 51605463), the Fundamental Research Funds for the Central Universities (no. WK2480000002, WK6030000007, and WK2090090018), the China Postdoctoral Science Foundation (no. 2016 M590578, 2016 M602027), the Chinese Academy of Sciences Instrument Project (YZ201566) and the “Chinese Thousand Young Talents Program”.

References

- 1 I. B. Ivshina, M. S. Kuyukina, A. V. Krivoruchko, A. A. Elkin, S. O. Makarov, C. J. Cunningham, T. A. Peshkur, R. M. Atlas and J. C. Philp, *Environ. Sci.: Processes Impacts*, 2015, **17**, 1201.
- 2 X. Y. Zhang, Z. Li, K. S. Liu and L. Jiang, *Adv. Funct. Mater.*, 2013, **23**, 2881.
- 3 N. Liu, Y. Z. Cao, X. Lin, Y. N. Chen, L. Feng and Y. Wei, *ACS Appl. Mater. Interfaces*, 2014, **6**, 12821.
- 4 J. Liu, L. Wang, F. Y. Guo, L. L. Hou, Y. Chen, J. C. Liu, N. Wang, Y. Zhao and L. Jiang, *J. Mater. Chem. A*, 2016, **4**, 4365.

- 5 Z. X. Xue, S. T. Wang, L. Lin, L. Chen, M. J. Liu, L. Feng and L. Jiang, *Adv. Mater.*, 2011, **23**, 4270.
- 6 L. Feng, Z. Y. Zhang, Z. H. Mai, Y. M. Ma, B. Q. Liu, L. Jiang and D. B. Zhu, *Angew. Chem., Int. Ed.*, 2004, **43**, 2012.
- 7 J. Y. Yun, F. A. Khan and S. Baik, *ACS Appl. Mater. Interfaces*, 2017, **9**, 16694.
- 8 H. C. Bi, X. Xie, K. B. Yin, Y. L. Zhou, S. Wan, L. B. He, F. Xu, F. Banhart, L. T. Sun and R. S. Ruoff, *Adv. Funct. Mater.*, 2012, **22**, 4421.
- 9 C. Wu, X. Y. Huang, X. F. Wu, R. Qian and P. K. Jiang, *Adv. Mater.*, 2013, **25**, 5658.
- 10 J. Ge, Y. D. Ye, H. B. Yao, X. Zhu, X. Wang, L. Wu, J. L. Wang, H. Ding, N. Yong, L. H. He and S. H. Yu, *Angew. Chem., Int. Ed.*, 2014, **53**, 3612.
- 11 Z. Shi, W. B. Zhang, F. Zhang, X. Liu, D. Wang, J. Jin and L. Jiang, *Adv. Mater.*, 2013, **25**, 2422.
- 12 L. R. Shi, K. Chen, R. Du, A. Bachmatiuk, M. H. Rümmele, K. W. Xie, Y. Y. Huang, Y. F. Zhang and Z. F. Liu, *J. Am. Chem. Soc.*, 2016, **138**, 6360.
- 13 F. J. Wang, S. Lei, M. S. Xue, J. F. Ou, C. Q. Li and W. Li, *J. Phys. Chem. C*, 2014, **118**, 6344.
- 14 Z. J. Wang, Y. Wang and G. J. Liu, *Angew. Chem., Int. Ed.*, 2016, **128**, 1313.
- 15 J. C. Gu, P. Xiao, J. Chen, J. W. Zhang, Y. J. Huang and T. Chen, *ACS Appl. Mater. Interfaces*, 2014, **6**, 16204.
- 16 Y. Z. Zhu, D. Wang, L. Jiang and J. Jin, *NPG Asia Mater.*, 2014, **6**, e101.
- 17 A. K. Kota, G. Kwon, W. Choi and J. M. Mabry, *Nat. Commun.*, 2012, **3**, 1025.
- 18 M. M. Tao, L. X. Xue, F. Liu and L. Jiang, *Adv. Mater.*, 2014, **26**, 2943.
- 19 F. Zhang, W. B. Zhang, Z. Shi, D. Wang, J. Jin and L. Jiang, *Adv. Mater.*, 2013, **25**, 4192.
- 20 J. L. Yong, F. Chen, Q. Yang, H. Bian, G. Q. Du, C. Shan, J. L. Huo, Y. Fang and X. Hou, *Adv. Mater. Interfaces*, 2016, **3**, 1500650.
- 21 A. K. An, J. X. Guo, E. J. Lee, S. Jeong, Y. H. Zhao, Z. K. Wang and T. O. Leiknes, *J. Membr. Sci.*, 2017, **525**, 57.
- 22 Y. H. Zhao, M. Zhang and Z. K. Wang, *Adv. Mater. Interfaces*, 2016, **3**, 1500664.
- 23 Z. L. Chu, Y. J. Feng and S. Seeger, *Angew. Chem., Int. Ed.*, 2015, **54**, 2328.
- 24 X. F. Gao, L. P. Xu, Z. X. Xue, L. Feng, J. T. Peng, Y. Q. Wen, S. T. Wang and X. J. Zhang, *Adv. Mater.*, 2014, **26**, 1771.
- 25 Q. L. Ma, H. F. Cheng, A. G. Fane, R. Wang and H. Zhang, *Small*, 2016, **12**, 2186.
- 26 J. Ge, H. Y. Zhao, H. W. Zhu, J. Huang, L. A. Shi and S. H. Yu, *Adv. Mater.*, 2016, **28**, 10459.
- 27 H. C. Bi, X. Huang, X. Wu, X. H. Cao, C. L. Tan, Z. Y. Yin, X. H. Lu, L. T. Sun and H. Zhang, *Small*, 2014, **10**, 3544.
- 28 B. Chao, Q. L. Ma, C. L. Tan, T. T. Lim, L. Huang and H. Zhang, *Small*, 2015, **11**, 3319.
- 29 G. Q. Li, H. Fan, F. F. Ren, C. Zhou, Z. Zhang, B. Xu, S. Z. Wu, Y. L. Hu, W. L. Zhu, J. W. Li, Y. S. Zeng, X. H. Li, J. R. Chu and D. Wu, *J. Mater. Chem. A*, 2016, **4**, 18832.
- 30 S. Ye, Q. Cao, Q. S. Wang, T. Y. Wang and Q. Peng, *Sci. Rep.*, 2016, **6**, 37591.
- 31 L. Aurélie and D. Quéré, *Nat. Mater.*, 2003, **2**, 457.
- 32 C. Journet, S. Moulinet, C. Ybert, S. T. Purcell and L. Bocquent, *Europhys. Lett.*, 2005, **71**, 104.
- 33 X. Y. Li, D. Hu, K. Huang and C. F. Yang, *J. Mater. Chem. A*, 2014, **2**, 11830.